International Journal of Applied Science and Engineering
2013. 11, 4: 343-360

Critical Study of Open-ended Coaxial Sensor by Finite Element Method (FEM)

M. A. Jusoh[a*], Z. Abbas[b], M. A. A. Rahman[b], C. E. Meng[c], M. F. Zainuddin[b], and F. Esa[b]

[a] *Faculty of Industrial Sciences and Technology, Universiti Malaysia Pahang, Malaysia*
[b] *Department of Physics, Faculty of Science, Universiti Putra Malaysia, Selangor, Malaysia*
[c] *School of Mechatronic Engineering, Universiti Malaysia Perlis, Malaysia*

Abstract: This paper describes the critical study of open ended coaxial sensor using simulation technique by finite element method. The simulation includes the finding of cutoff wavenumber at each mode and was compared to analytical method. The simulation was also performed in finding the minimum thickness requirement for sample and the influencing parameters of coaxial probe performance. The simulation was carried out using COMSOL software.

Keywords: Open ended coaxial; finite element method; COMSOL.

1. Introduction

An open ended coaxial line has been used by many researchers as a sensor of nondestructive testing for measuring moisture content [1-2] and complex permittivity [3-4] of materials. In this method, the sample is placed against an open end of a coaxial line and its reflection coefficient is measured. The complex permittivity of the material is then calculated using an equivalent admittance model of the coaxial sensor [1]. A coaxial line having inner and outer radii a and b, respectively, filled with a lossless homogeneous dielectric having a relative permittivity is terminated in the plane z=0 into a flat metallic flange extending theoretically to infinity in the transverse direction [5].The material terminating the aperture is assumed to be homogeneous, isotropic, linear, and nonmagnetic, of complex permittivity extending to infinity. A static capacitance C, due to the fringing fields excited by the TEM fields of the line over the aperture. The schematic diagram of open ended coaxial sensor with sample was shown in Figure 1. The critical studies of open ended coaxial sensor have been discussed by Grant [3]. But his paper not thoroughly discussed the electric field distribution inside the coaxial line. Knowing the electric field distribution inside coaxial line is very important especially in higher order modes and some analytical models were not considering higher order modes. Using numerical technique such as finite element method (FEM), the electric and magnetic field at higher order modes can be easily determined.

2. Theory

A coaxial line having inner and outer radii a and b, respectively, filled with a lossless homogeneous dielectric. The wavenumber for coaxial waveguide can be obtained with the root

* Corresponding author; e-mail: ashryj@gmail.com

© 2013 Chaoyang University of Technology, ISSN 1727-2394

Received 12 July 2012
Revised 28 September 2012
Accepted 25 April 2013

of Bessel-neumann and its derivative combination respectively whereby the cutoff wavenumber can be found at intercept between first and second term as shown in Equation (1) and (2).

$$\left.\begin{matrix} J_m'(ka)Y_m'(kb) \\ J_m'(kb)Y_m'(ka) \end{matrix}\right\} TE_{mn} \tag{1}$$

and

$$\left.\begin{matrix} J_m(ka)Y_m(kb) \\ J_m(kb)Y_m(ka) \end{matrix}\right\} TM_{mn} \tag{2}$$

COMSOL is a generic finite element method solver based on custom partial differential equations (PDE). The basic solving procedure in COMSOL includes geometric modeling, physical modeling, mesh generation, FEM matrix assembly, matrix solving and post processing. For a general TE-wave harmonic problem, COMSOL solve for the E_z field component. COMSOL solves the following equation

$$\nabla \times \left(\mu_r^{-1} \nabla \times e\right) - k_o^2 \varepsilon_{rc} e = 0 \tag{3}$$

where μ_r is the relative permeability and ε_{rc} is the relative permittivity. The matrix assembly leads to the form:

$$\begin{bmatrix} K & N^T \\ N & 0 \end{bmatrix} \begin{bmatrix} E \\ \Lambda \end{bmatrix} = \begin{bmatrix} L \\ M \end{bmatrix} \tag{4}$$

which, after further transformation, produces the standard FEM formulation ***Ke*= *b*** [7].

For 2-D problems, direct UMFPACK method was chosen to solve these problems with relatively small matrix size, (with very high speed, usually in seconds for meshes about several thousand elements). For large problems like 3-D problems, COMSOL implements iterative methods with LU pre-conditioner. These solutions are more time-consuming because of their large scale.

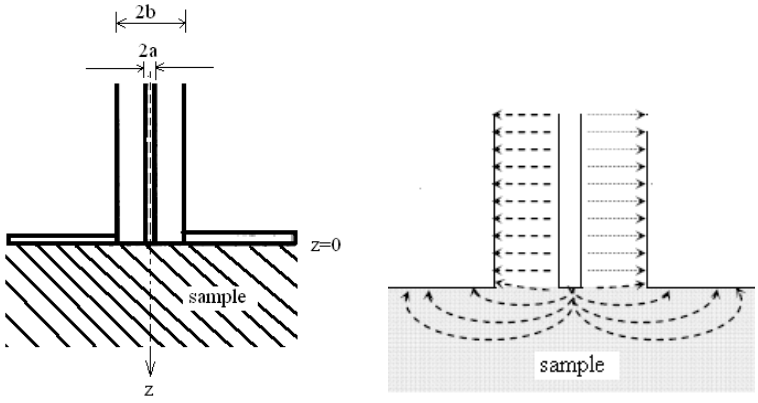

(a) (b)

Figure 1. Open ended coaxial sensor (a) schematic diagram; (b) electric field distribution [6]

3. Methodology

The FEM simulation of coaxial sensor and sample was implemented by using COMSOL

Multiphysics software. The geometry of coaxial waveguide was shown in Figure 2. The simulation was carried out by using quadrilateral form with 618 elements. The simulation was running by using 1.50 GHz processors with 760Mb RAM. In two-dimensional FEM modeling, the most popular element shapes to be employed is triangles and quadrilaterals. The simulation was started with determination of wavenumber coaxial waveguide. In COMSOL, the results were calculated using higher order modes which are neglected by quasi TEM that was calculated from analytical method. The simulation results then were compared with analytical results. Then, the aspect ratio of coaxial waveguide was simulated so that the optimum performance of coaxial sensor can be recognized. The boundary condition for open ended coaxial sensor and sample was shown in Figure 3.

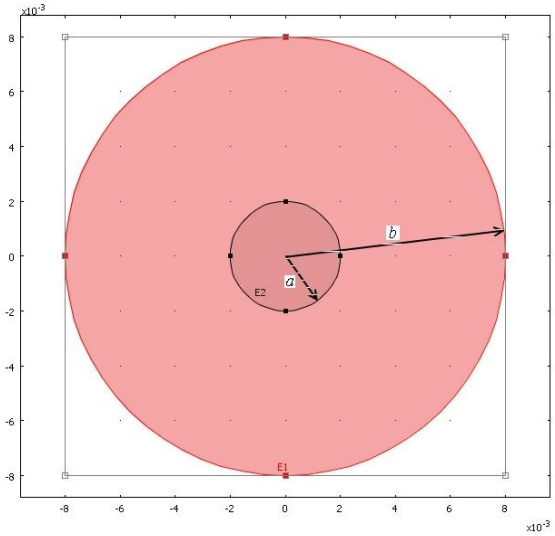

Figure 2. Schematic diagram of coaxial waveguide (radius, a=2mm b=8mm)

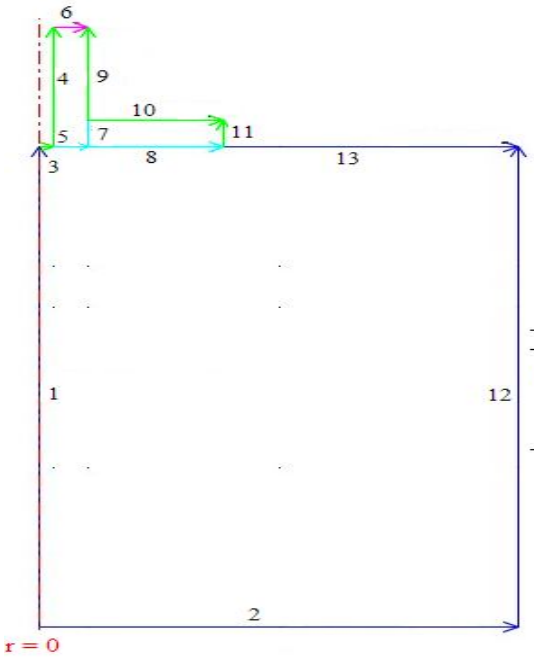

Condition	Boundaries
Axial Symmetry	1
Perfect Electric Conductor	3, 4, 9, 10, 11
Matched Boundary	2, 12, 13
Port	6
Continuity	5,7, 8

Figure 3. Boundary condition for open ended coaxial sensor and sample

4. Results and discussion

4.1. Cutoff wave number for coaxial waveguide

The simulation was performed at perpendicular TE or TM mode situation whereby the eigenvalue easily can be determined by using COMSOL software. To ensure that the simulation was correct, the simulation result was compared with analytical equation as discussed above. It is found that the simulation results are in good agreement with analytical results as shown in Table 1. Figures 4, 5 and 6 show the electric field distribution while Figure 7 and 8 show the magnetic field distribution at different mode in open ended coaxial sensor. It is found that the higher of mode gives the higher of cutoff wave number for coaxial waveguide whereby as well known, TM modes in coaxial are higher order modes.

In COMSOL, the eigenvalue is defined as $-\lambda = \beta^2$. While and a and b are radius of inner and outer conductor respectively. The cutoff wavenumber can be found using

$$k_c = \sqrt{\gamma^2 + k_0^2} \tag{5}$$

where γ is a propagation constant $\gamma = \alpha + j\beta$ and $k_0 = \dfrac{2\pi f}{c}$ where c is a speed of light. Assuming that $\alpha = 0$, then the propagation constant is $\gamma = j\beta$.

Then, the cutoff wavenumber can be written as

$$k_c = \sqrt{(j\beta)^2 + k_0^2} \tag{6}$$

$$k_c = \sqrt{\lambda + k_0^2} \tag{7}$$

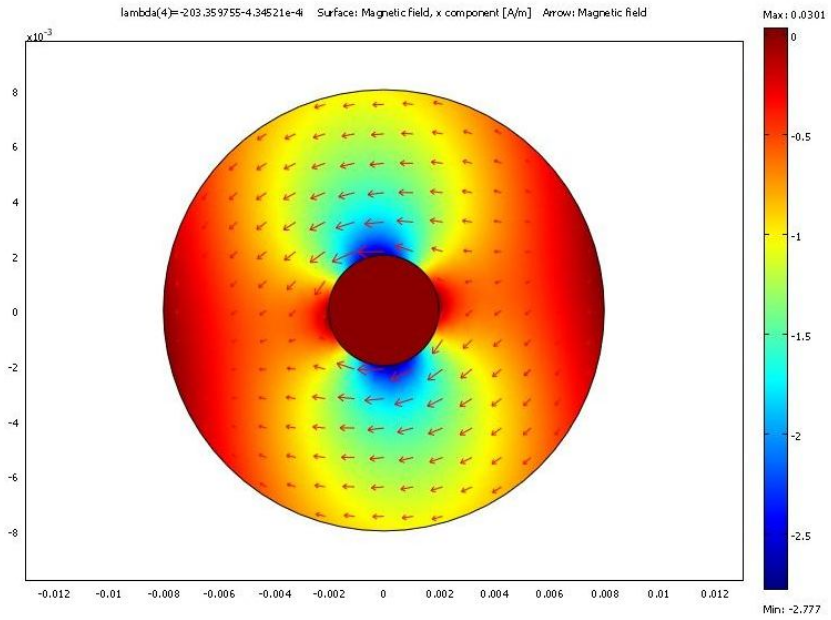

Figure 4. Magnetic field distribution at TE_{11} mode for coaxial waveguide

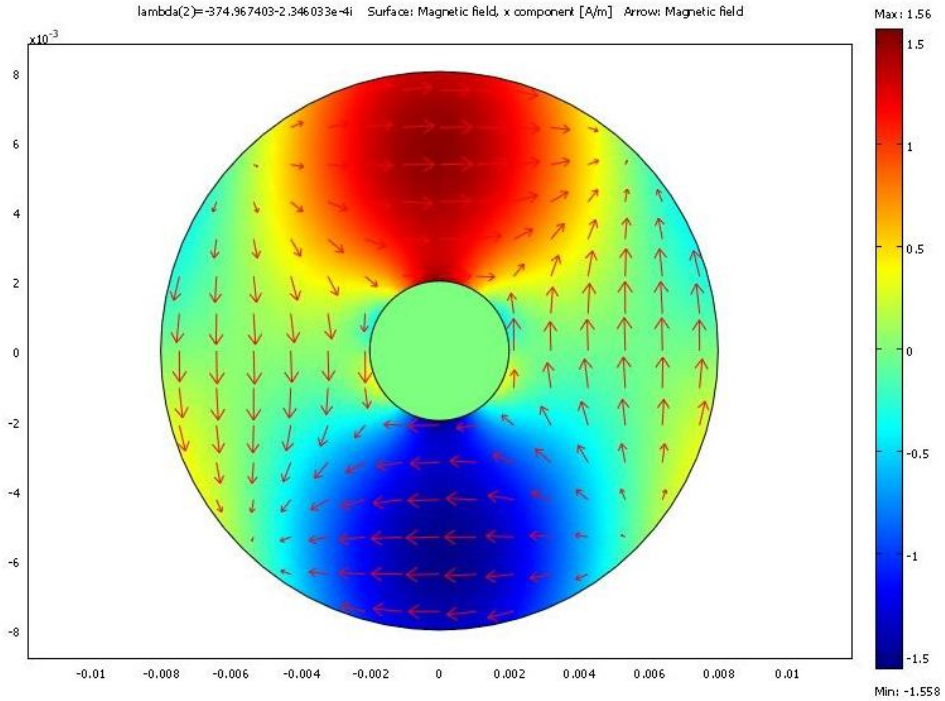

Figure 5. Magnetic field distribution at TE_{21} mode for coaxial waveguide

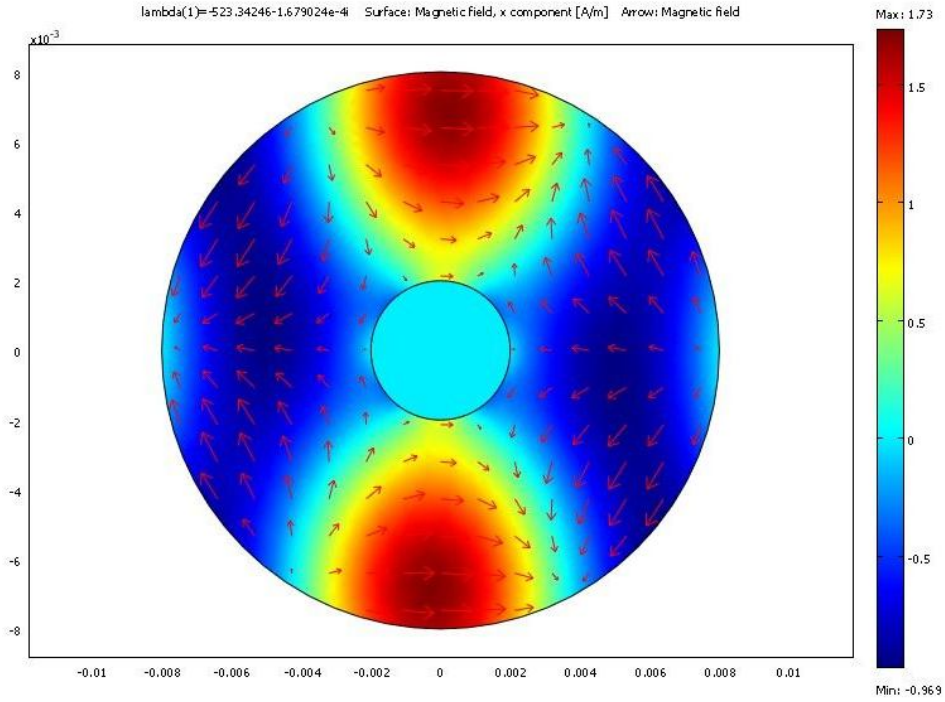

Figure 6. Magnetic field distribution at TE_{31} mode for coaxial waveguide

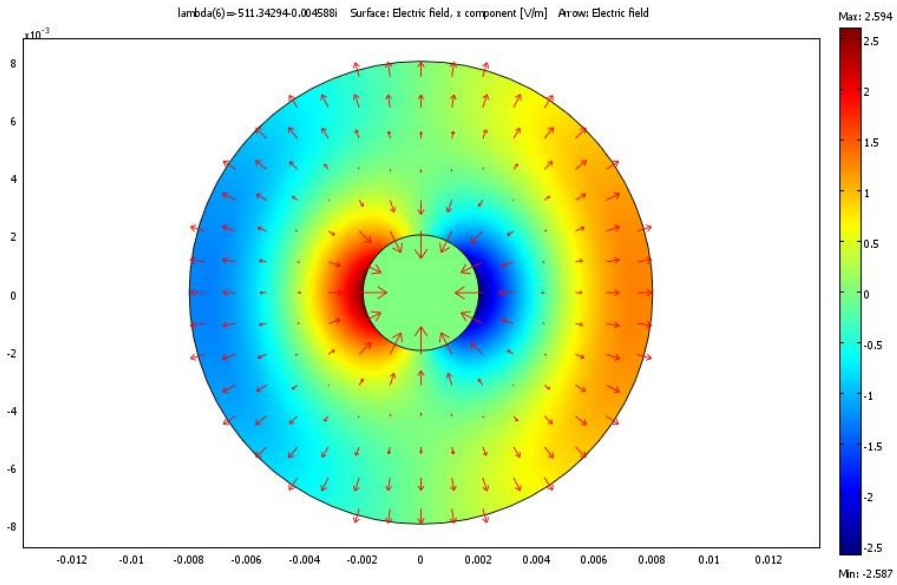

Figure 7. Magnetic field distribution at TM_{01} mode for coaxial waveguide

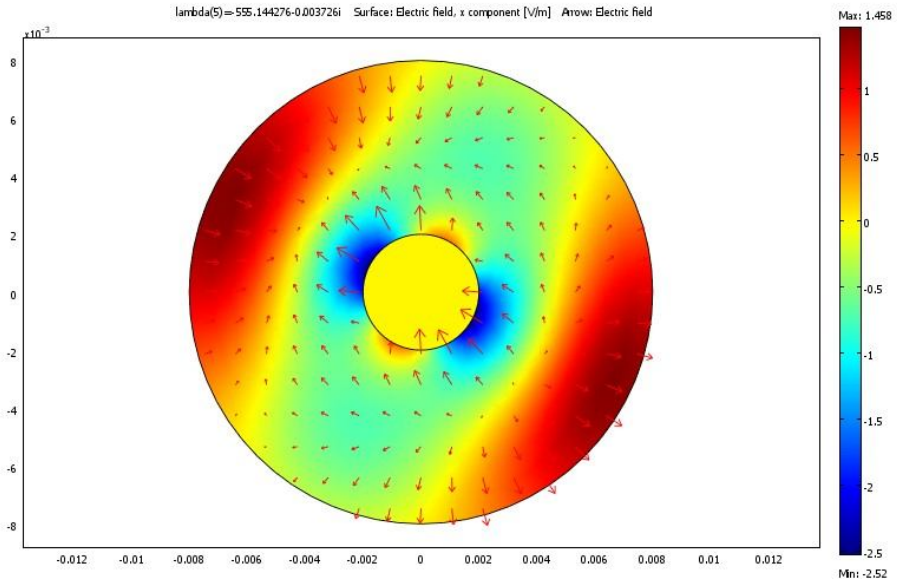

Figure 8. Magnetic field distribution at TM_{11} mode for coaxial waveguide

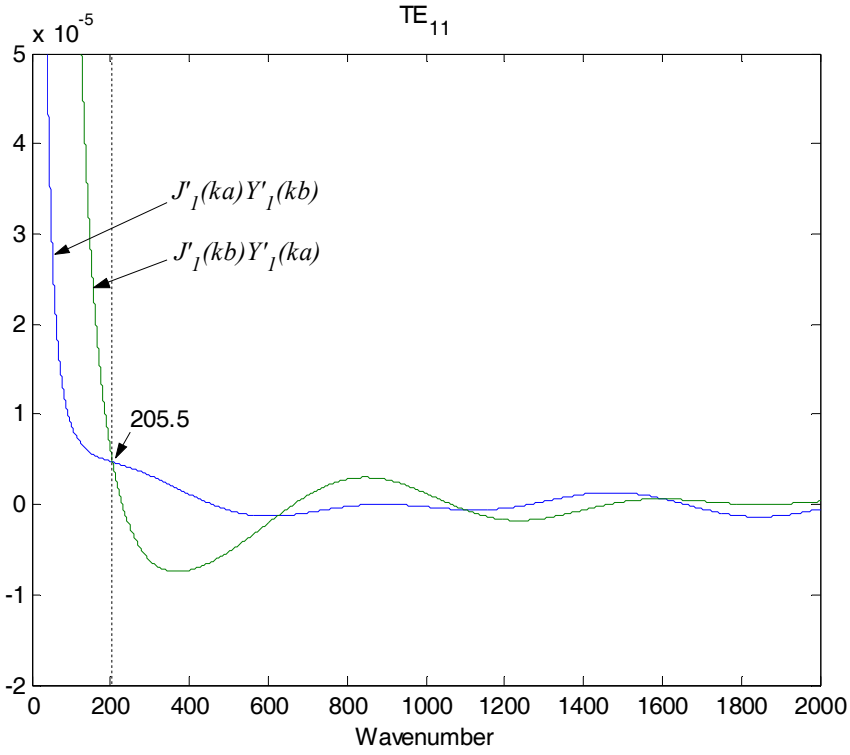

Figure 9. Cutoff wavenumber for coaxial waveguide at TE_{11}

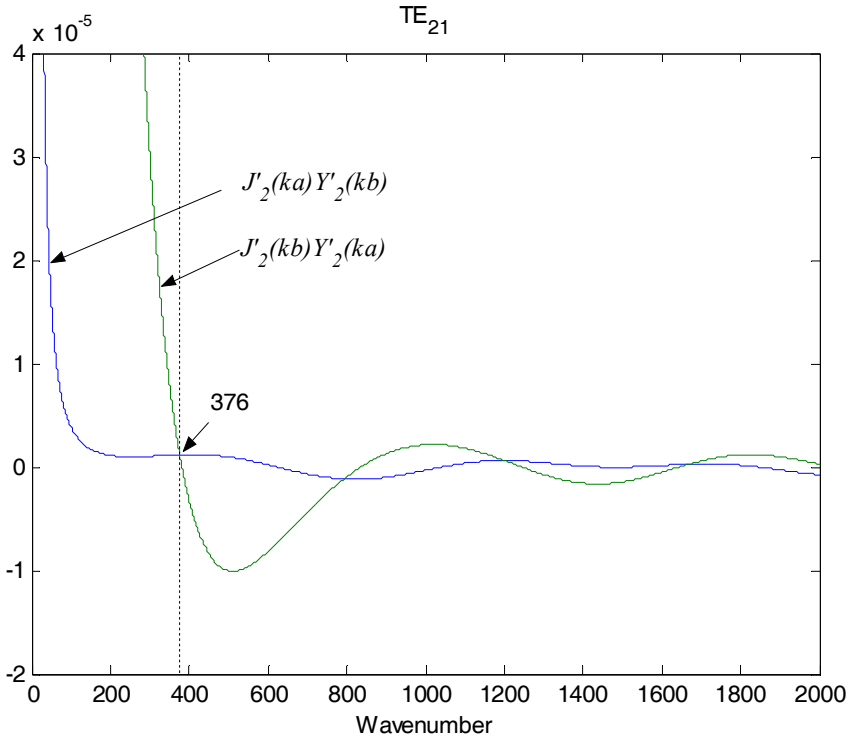

Figure 10. Cutoff wavenumber for coaxial waveguide at TE_{21}

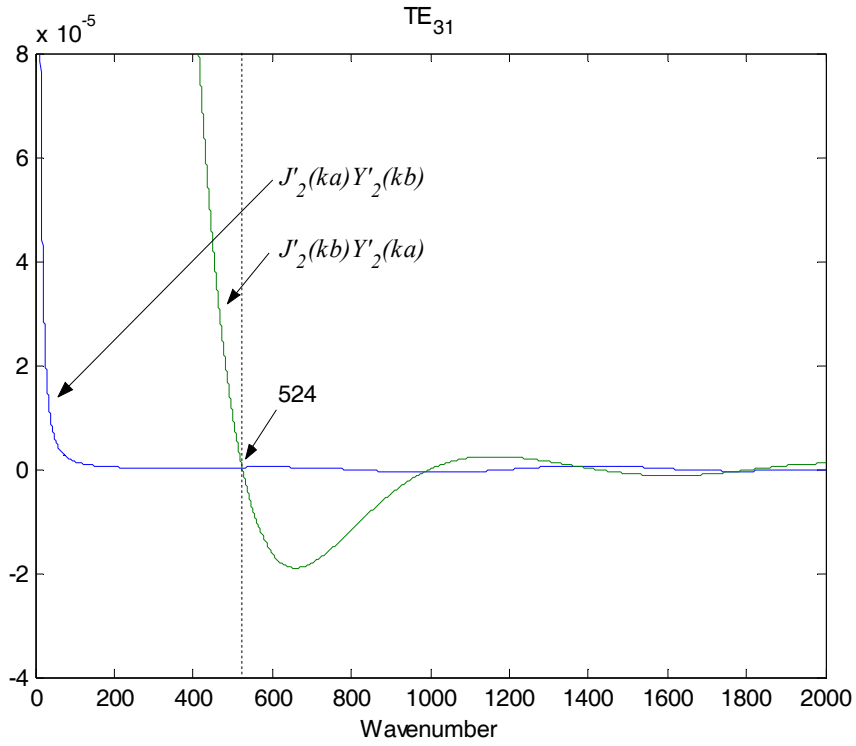

Figure 11. Cutoff wavenumber for coaxial waveguide at TE_{31}

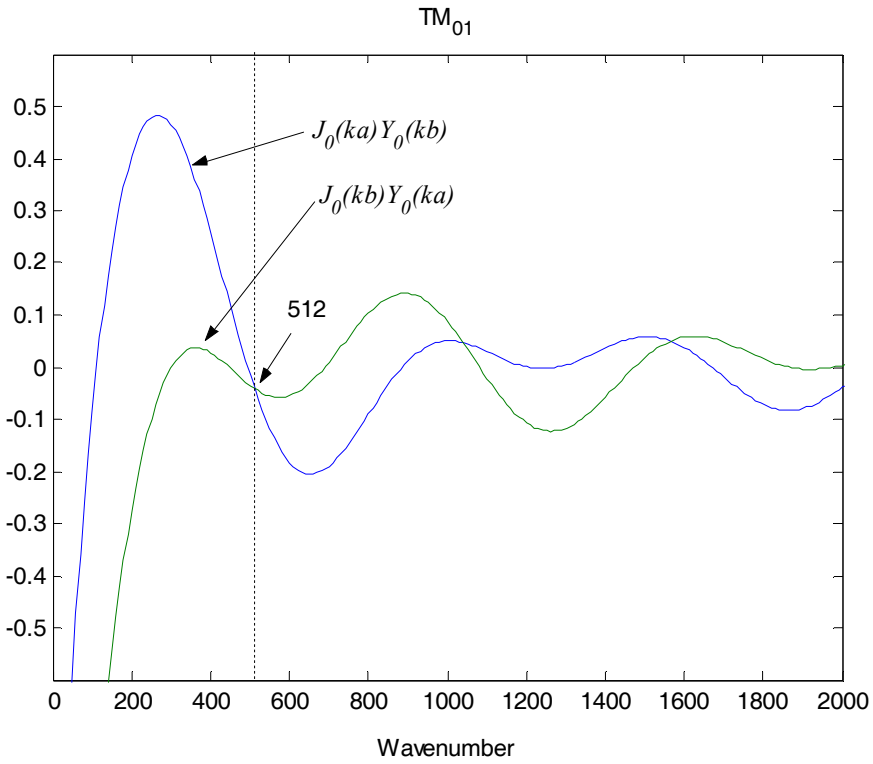

Figure 12. Cutoff wavenumber for coaxial waveguide at TM_{01}

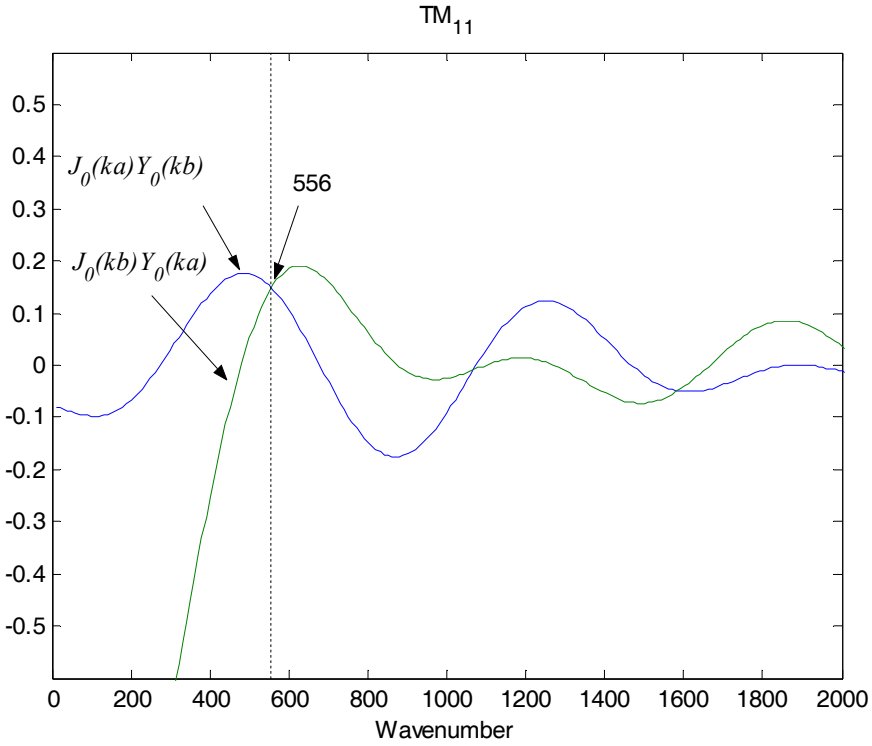

Figure 13. Cutoff wavenumber for coaxial waveguide at TM_{11}

Table 1. Cutoff wave number, k_c for coaxial waveguide

Mode		k_c		eigenvalue
TE	TM	Analytical	COMSOL	COMSOL
11		205.5	204.4354	41355.1899
21		376	375.5519	140600.5533
31		524	523.7614	273887.3304
	01	512	511.7717	261471.6238
	11	556	555.5392	308185.1537

a=2mm; b/a=4

4.2. Thickness requirement for sample

The minimum requirement for thickness of sample is very important to ensure that the reflection is only due to that sample. The electric field coming out from open ended coaxial sensor as well known is in fringing field form. The maximum distance of electric field that will propagate into sample is a minimum requirement for that sample. The propagation of wave into sample is strongly related to the permittivity of that sample which is the higher of permittivity of sample give a smaller of electric field that will propagate into sample. In this simulation, the permittivity of sample was considered as small as possible so that the electric field that will propagate is far enough to that sample. The simulation begins with drawing geometry of coaxial sensor and sample as shown in Figure 14. Since the geometry of sensor is in symmetry form, then the geometry of sensor as shown in Figure 14 can be simplified as the geometry as shown in Figure 15. The number of element that will be used in this simulation is 4454 quadrilateral

elements since the results give a smallest relative error when it was compared with experimental results. The quadrilateral element was used since the geometry of sensor is rectangular form while the triangles elements are quite convenient for mesh generation, mesh transitions and rounding up corners.

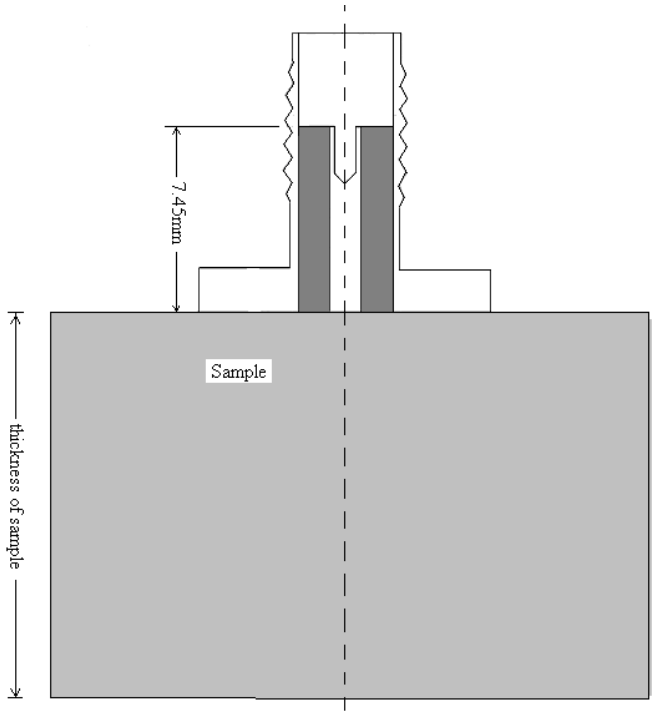

Figure 14. Schematic diagram for open ended coaxial sensor measurement

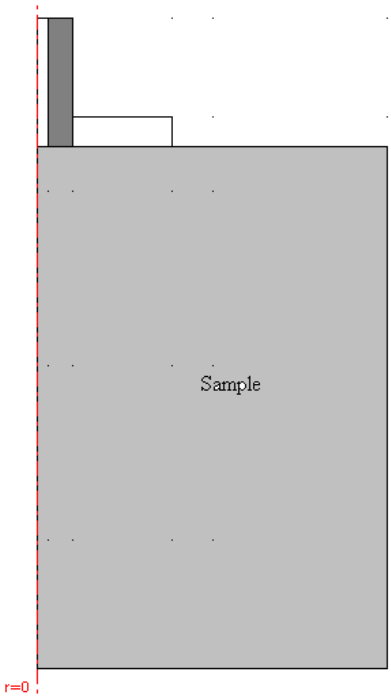

Figure 15. Drawing mode in axial symmetry (2D) for simulation of sample by COMSOL

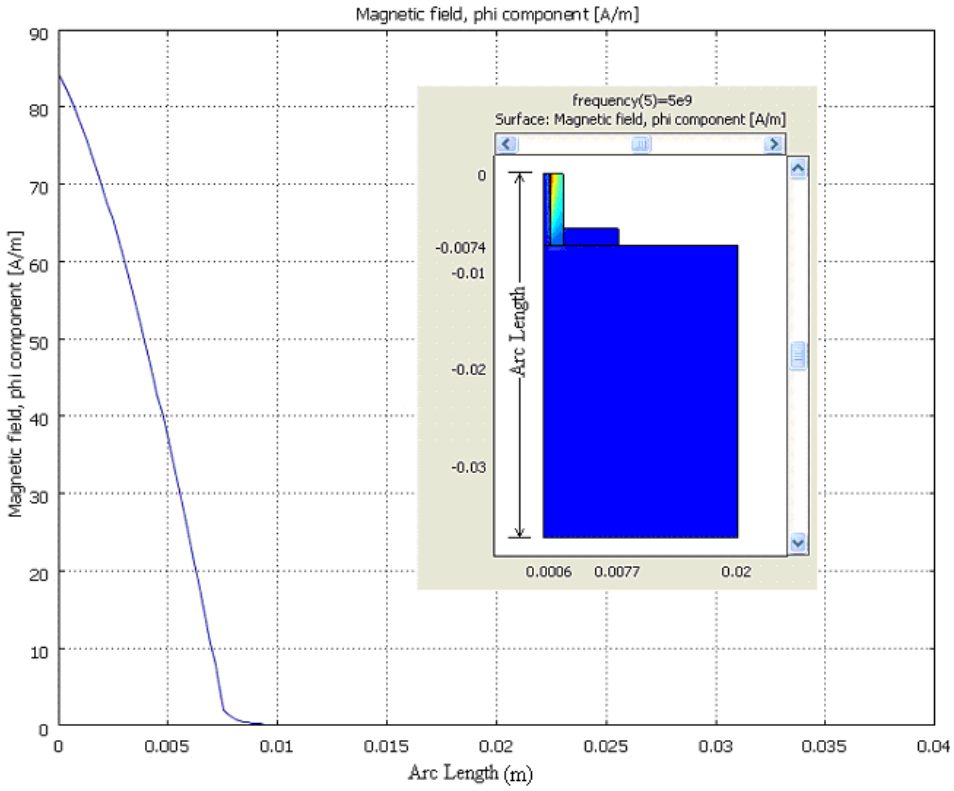

Figure 16. Magnetic field as a function of arc length for $\varepsilon = 1$

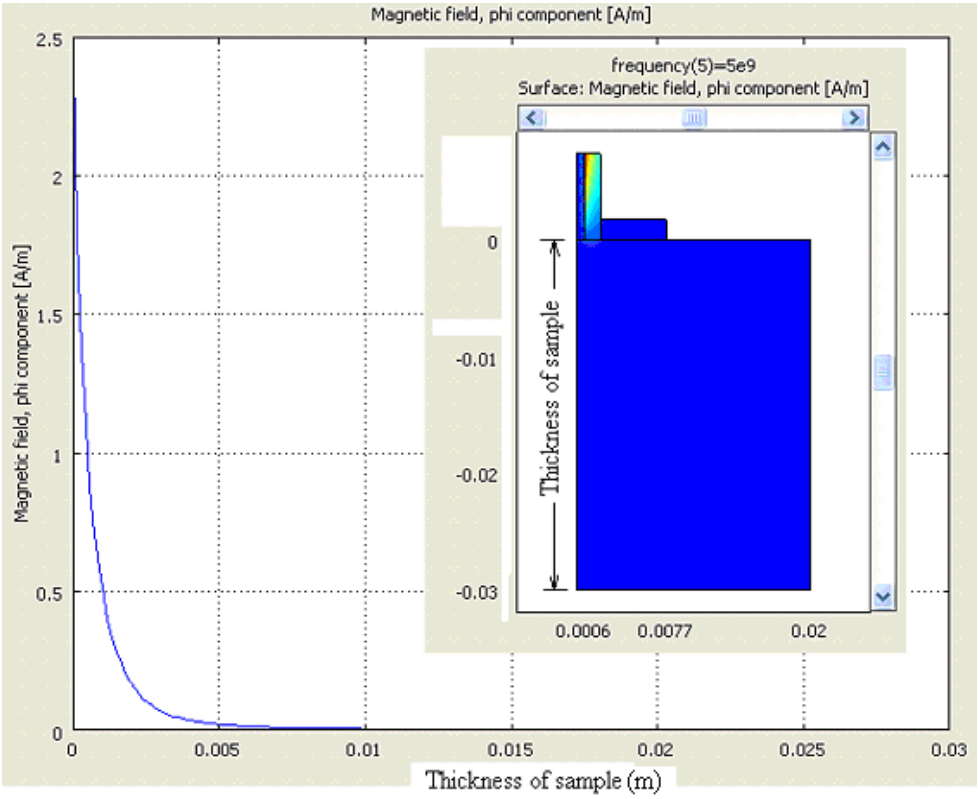

Figure 17. Magnetic field as a function of sample thickness for $\varepsilon = 1$

Figure 17 shows that the magnetic field as a function of sample thickness for dielectric permittivity is 1. It is clearly shows that the magnetic field decreases with thickness of sample. It is observed that when the thickness sample exceeds 10 mm, the measured magnitude and phase of reflection coefficient is unchanged. The minimum thickness of sample is depends on the permittivity of sample and outer diameter of coaxial sensor as formulated in Equation (8).

$$\text{Minimum thickness} = \frac{\text{Outer diameter}}{\sqrt{\varepsilon^*}} \tag{8}$$

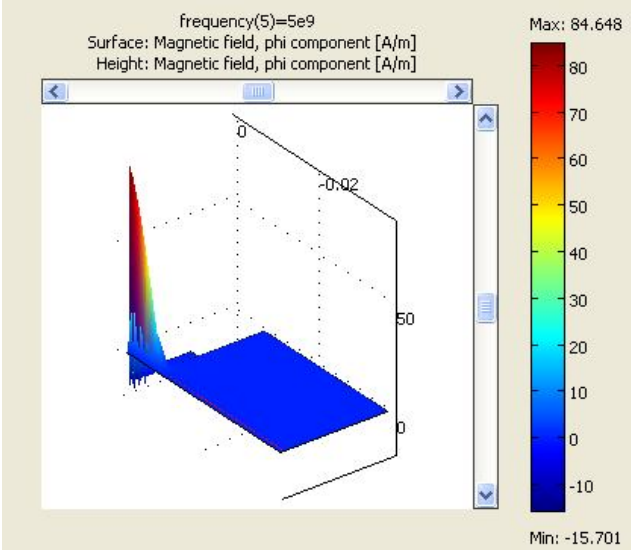

Figure 18. 3D simulation for open ended coaxial sensor

Figure 18 shows that the 3D simulation for open ended coaxial sensor for air sample whereby the magnetic distribution shows that the magnetic field is higher at open ended coaxial sensor where the red color shows the highest value of magnetic field compared to blue color.

4.3. Influence parameter of coaxial probe performance

In this section, the effect of aspect ratio between outer, *b* and inner, *a* diameter and also the effect of the length *l* of the inner conductor will be discussed thoroughly. The schematic diagram of open ended coaxial sensor with inner and outer conductor was shown in Figure 19.

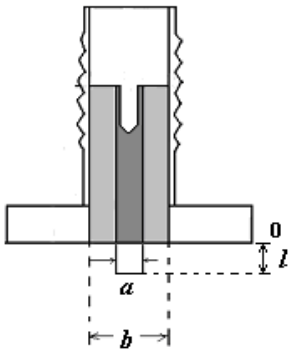

Figure 19. Schematic diagram of open ended coaxial sensor with inner, *a* and outer, *b* diameter as well as the length, *l* of inner conductor

4.3.1. The effect of aspect ratio (b/a)

This section will be discussed about the effect of aspect ratio for performance of open ended coaxial sensor. Several aspect ratios were selected based on the types of coaxial sensor in market. There are 3.333, 3.154, 2.36, 2.0 and 1.57. The simulation was performed with inner conductor diameter, ***a*** is 0.65 mm. The detail of aspect ratio was described in Table 2.

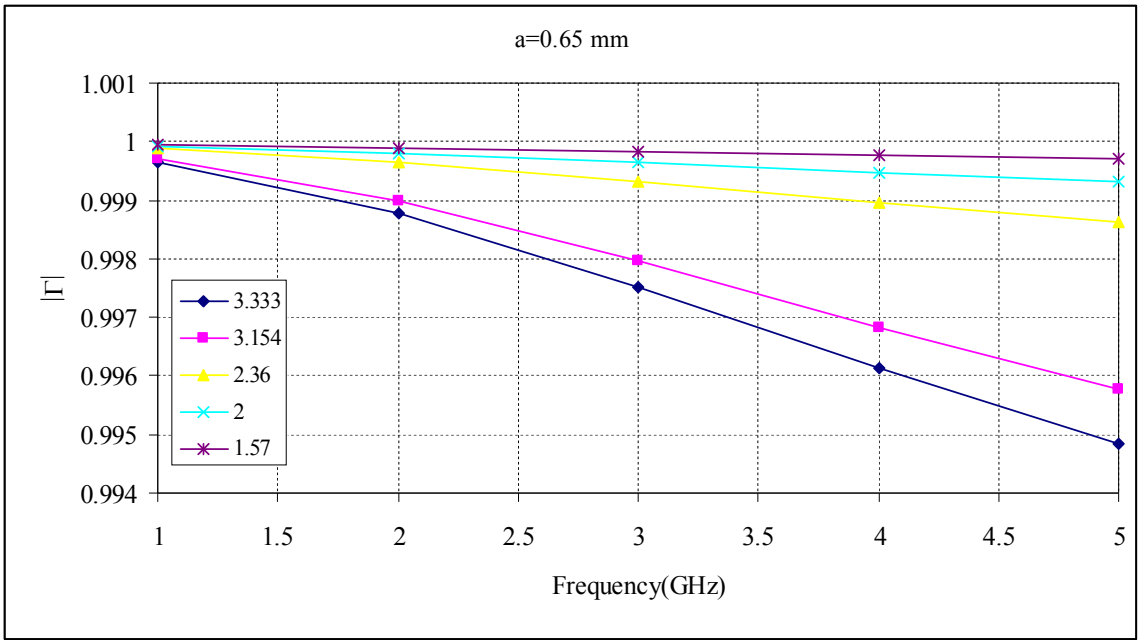

Figure 20. Relationship between magnitude of reflection coefficient and frequency for various aspect ratios

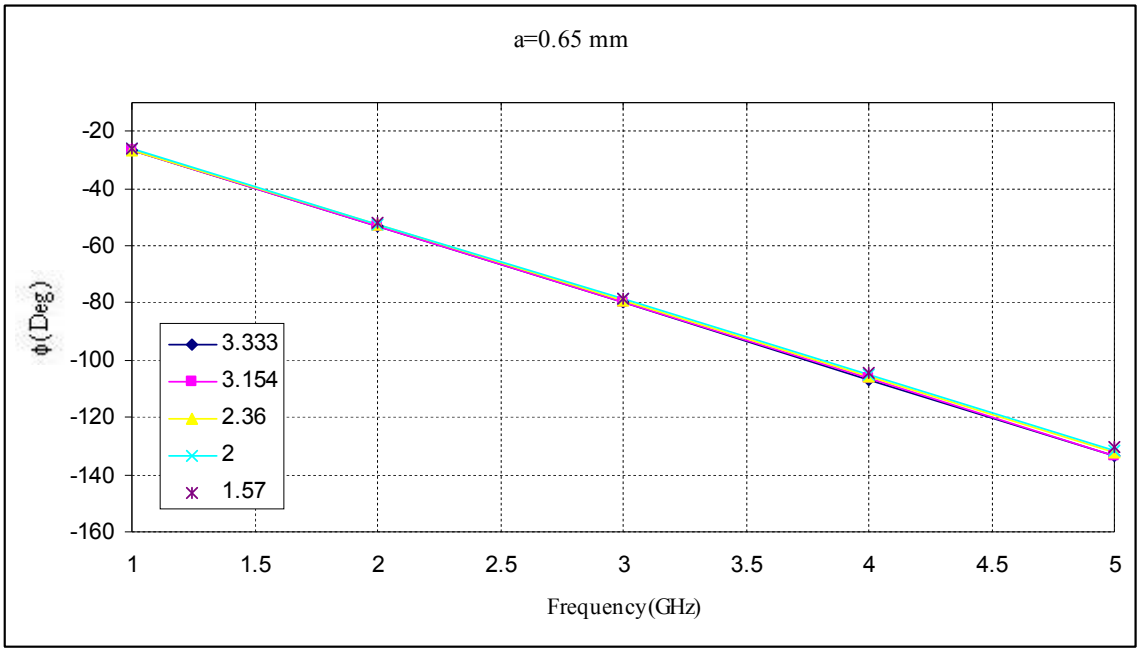

Figure 21. Relationship between phase of reflection coefficient and frequency for various aspect ratio

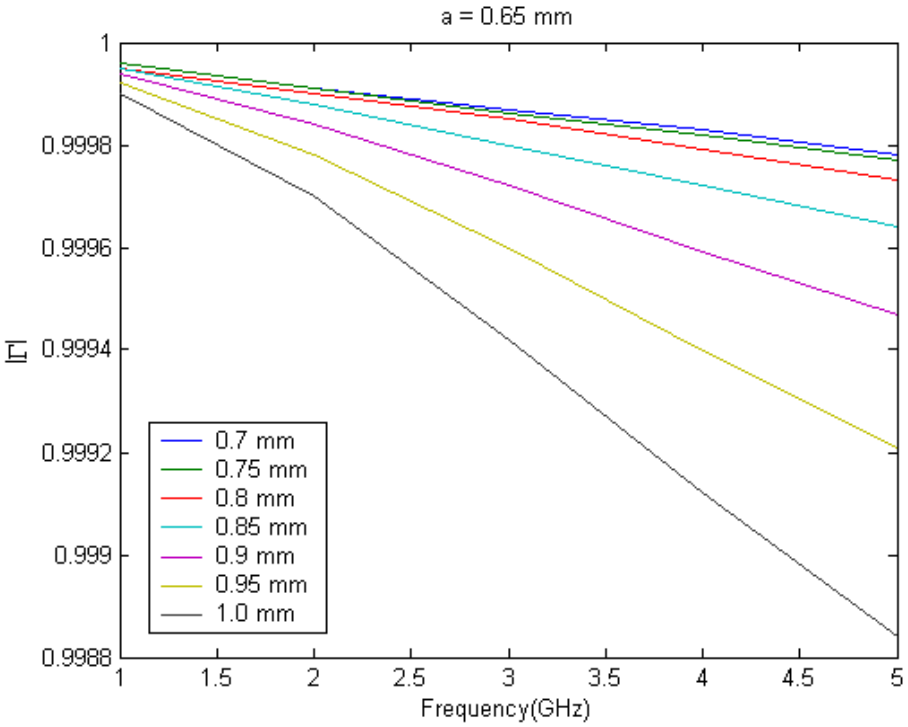

Figure 22. Relationship between phase of reflection coefficient and frequency for various radius of outer conductor

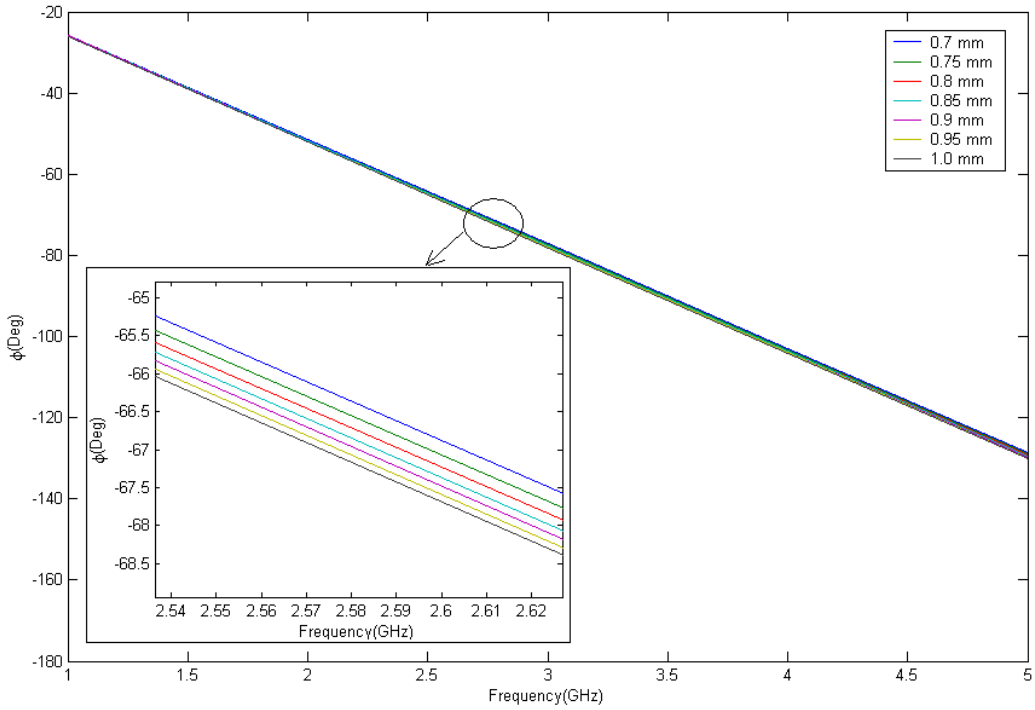

Figure 23. Relationship between phase of reflection coefficient and frequency for various radius of outer conductor

Table 2. Outer and inner diameter of coaxial sensor

Outer diameter, *b* (mm) (a=0.65mm; *l*=0 mm)	Aspect ratio (b/a)
2.1665	3.333
2.0501	3.154
1.5340	2.36
1.3	2.0
1.0205	1.57

4.3.2. The effect of length *l* of the inner conductor

The effect of aspect ratio was discussed thoroughly in previous section. It was clearly seen that the best aspect ratio is 1.57 since the magnitude of reflection coefficient for air is close to 1. In this section, the effect of length of the inner conductor will be discussed in detailed. The schematic diagram of open ended coaxial with the length of inner conductor was shown in Figure 19. As shown in Figures 24 and 25, the shortest length of the inner conductor gives a good result whereby the result is going to close to 1 and 0 deg for magnitude and phase of reflection coefficient respectively.

4.3.3. Flange vs flangeless

The open ended coaxial sensor that was used in this study is a open ended coaxial sensor with flange. Figure 24 shows that the schematic diagram of open ended coaxial sensor with flange and without flange (flangeless). The simulation was performed with same mesh number of element. The simulation was performed for air sample and the result of reflection coefficient was compared for both sensors. As well known, the sensor with magnitude of reflection give a closest result to 1 or 0 dB is a best sensor in reflection measurement.

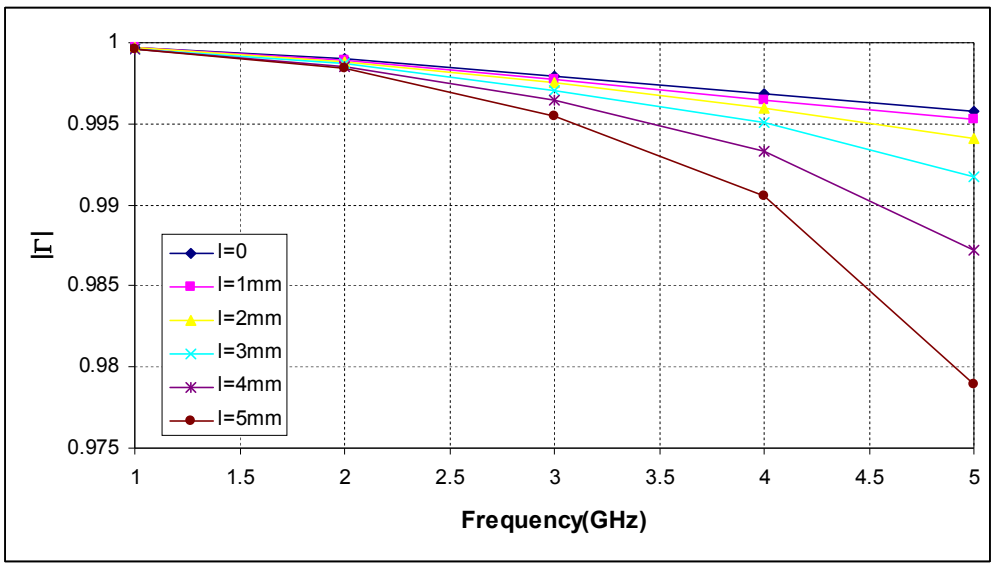

Figure 24. Relationship between magnitude of reflection coefficient and frequency

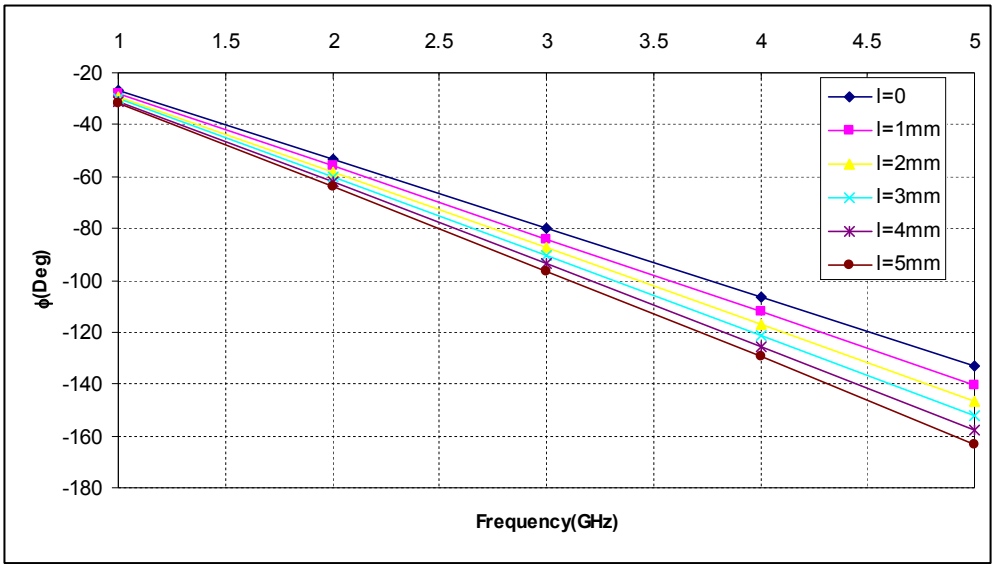

Figure 25. Relationship between phase of reflection coefficient and frequency for various lengths

Figure 26 shows that the relationship between reflection coefficients with frequency measured using open ended coaxial sensor with flange and without flange (flangeless). The results as shown in Figure 27 shows that the both sensor shows a same performance for a lower frequency but for a high frequency the sensor with flange shows a better result which is the magnitude of reflection coefficient is closest to 1.

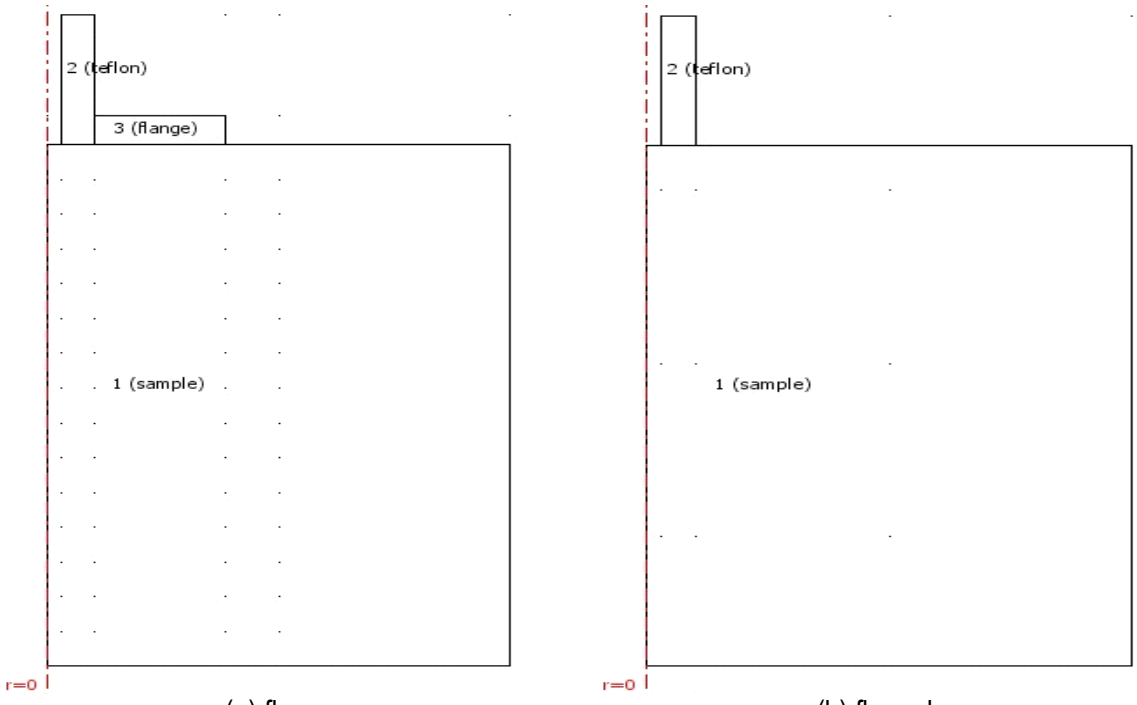

(a) flange (b) flangeless

Figure 26. Schematic diagram for open ended coaxial sensor (a) flange; (b) flangeless

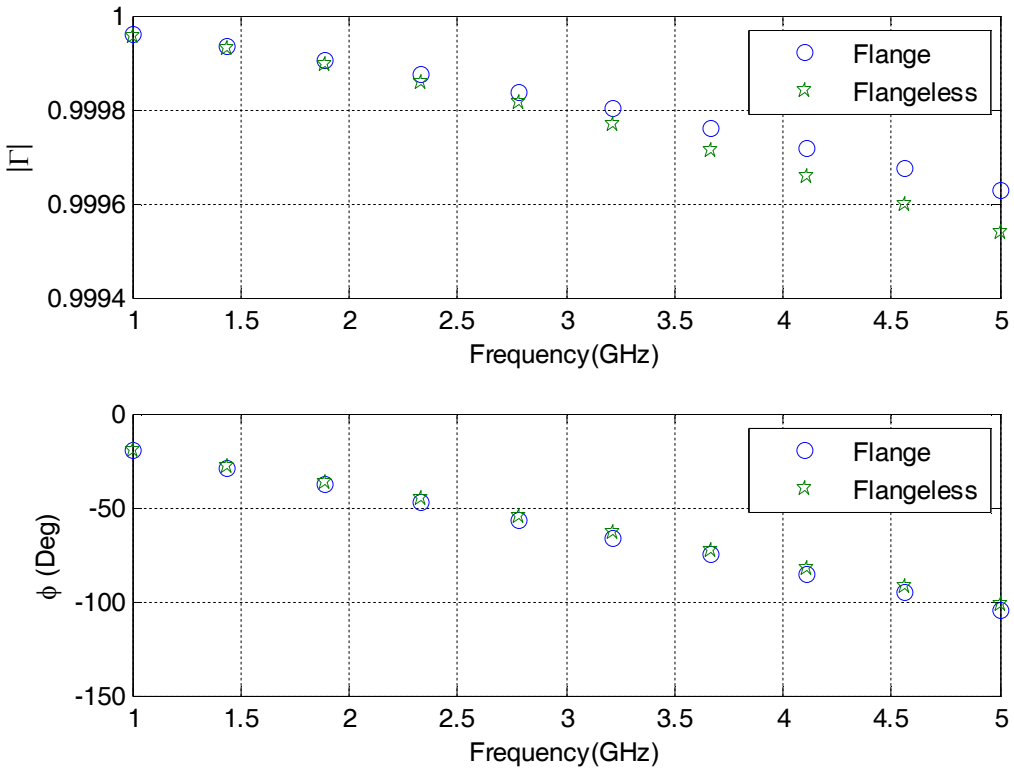

Figure 27. Magnitude and phase of reflection coefficient measured using open ended coaxial with flange and without flange (flangeless) for air

5. Conclusions

The simulation of open ended coaxial line has been performed using FEM and the results show a good agreement in finding cutoff wavenumber when compared with analytical results.

Acknowledgments

This research is funded by Ministry of Science and Technology under Research University Scheme (Project code: 05-01-07-0233RU).

References

[1] Abbas, Z., You, K. Y., Shaari, A. H., Zakaria, A., and Hassan, J. 2005. Fast and Accurate Technique for Determination of Moisture Content in Oil Palm Fruits Using Open-Ended Coaxial Sensor. *Japanese Journal of Applied Physics*, 44: 5272-5274.

[2] Abbas, Z., You K. Y., Shaari, A. H., Khalid, K., Hassan, J., and Saion, E. 2005. Complex Permittivity and Moisture Measurements of Oil Palm Fruits Using an Open-ended Coaxial Sensor. *Sensors Journal, IEEE*, 5, 6: 1281-1287.

[3] Grant, J. P., Clarke, R. N., Symm, G. T., and Spyrou, N. M. 1989. A Critical Study of the Open-Ended Coaxial Line Sensor Technique for RF and Microwave Complex Permittivity Measurements. *J. Phys. E: Sci. Instrum.*, 22: 757.

[4] Marsland, T. P. and Evans, S. 1987. Dielectric Measurement with an Open Ended Coaxial

Probe. *IEE Proceeding H.*, 134-349.
[5] Poumaropoulos, C. and Misra, D. 1993. A study on the coaxial aperture electromagnetic sensor and its application in material characterization. *IEEE Instrumentation and Measurement Technology Conference*, 52-55.
[6] You K. Y., Abbas Z., Khalid K., and Kong N. F. 2009. Improved formulation for admittance of thin and short monopole driving from coaxial line into dissipative media. *IEEE Antennas and Wireless Propagation Letters*, Vol. 8, 1246-1249.
[7] COMSOL®3.5 "*User Guide*". COMSOL, Inc., 8 New England Executive Park, Suite 310, Burlington, MA 01803. USA.